

SPECIFIC HEAT ON $\text{Sr}_2\text{Nb}_2\text{O}_7$ AND $\text{Sr}_2\text{Ta}_2\text{O}_7$

Y. Akishige^{1*}, H. Shigematsu¹, T. Tojo², H. Kawaji² and T. Atake²

¹Department of Physics, Faculty of Education, Shimane University, 1060 Nishikawatsu-cho, Matsue, Shimane 690-8504, Japan

²Materials and Structures Laboratory, Tokyo Institute of Technology, 4259 Nagatsuta-cho, Midori-ku, Yokohama, 226-8503, Japan

Specific heats on the single crystals of $\text{Sr}_2\text{Nb}_2\text{O}_7$, $\text{Sr}_2\text{Ta}_2\text{O}_7$ and $(\text{Sr}_{1-x}\text{Ba}_x)_2\text{Nb}_2\text{O}_7$ were measured in a wide temperature range of 2–600 K. Heat anomalies of a λ -type were observed at the incommensurate phase transition of T_{INC} (=495 K) on $\text{Sr}_2\text{Nb}_2\text{O}_7$ and at the super-lattice phase transition of T_{SL} (=443 K) on $\text{Sr}_2\text{Ta}_2\text{O}_7$; the transition enthalpies and the transition entropies were estimated. Furthermore, a small heat anomaly was observed at the low temperature ferroelectric phase transition of T_{LOW} (=95 K) on $\text{Sr}_2\text{Nb}_2\text{O}_7$. The transition temperature T_{LOW} decreases with increasing Ba content x and it vanishes for samples of $x > 2\%$.

Keywords: phase transition, specific heat, $(\text{Sr}_{1-x}\text{Ba}_x)_2\text{Nb}_2\text{O}_7$, $\text{Sr}_2\text{Nb}_2\text{O}_7$, $\text{Sr}_2\text{Ta}_2\text{O}_7$

Introduction

$\text{Sr}_2\text{Nb}_2\text{O}_7$ (abbreviate as SN) and $\text{Sr}_2\text{Ta}_2\text{O}_7$ (abbreviate as ST) belong to $\text{A}_2\text{B}_2\text{O}_7$ -type ferroelectrics with a layered perovskite structure. SN has a very high ferroelectric Curie temperature of $T_{\text{C}}=1615$ K [1], and takes place a normal incommensurate phase transition at $T_{\text{INC}}=493$ K [2, 3]. Above T_{C} the space group is assumed to be $\text{Cmcm}-D_{2h}^{17}$ in analogy to the paraelectric phase of ST, and below T_{C} the established space group is $\text{Cmc}2_1-\text{C}_{2v}^{12}$ [4]. Furthermore, SN takes place another ferroelectric phase transition at a low temperature of $T_{\text{LOW}} \approx 100$ K [5, 6]. Since SN has a low coercive field and a low dielectric constant at room temperature, it is promising for lead-free and non-volatile ferroelectric memory-devices based on FETs, as pointed out by Fujimori *et al.* [7]. On the other hand, ST shows a super-lattice phase transition at $T_{\text{SL}}=443$ K [3, 8], and a ferroelectric phase transition at $T_{\text{C}}=166$ K [1, 8]. In a solid solution of $\text{Sr}_2\text{Nb}_2\text{O}_7$ and $\text{Sr}_2\text{Ta}_2\text{O}_7$, the ferroelectric Curie temperature T_{C} decreases steeply from 1615 to 166 K with increasing Ta content [1]. By contrast, the incommensurate phase transition temperature T_{INC} changes little even if the Ta content increases, and the T_{INC} connects to the super-lattice phase transition temperature T_{SL} of ST [9]. Recently, we have investigated a new system of $(\text{Sr}_{1-x}\text{Ba}_x)_2\text{Nb}_2\text{O}_7$ and found that the phase transitions at T_{INC} and T_{LOW} decrease with increasing Ba content x and disappear near $x=2-4\%$ [10, 11]. As for the specific heat C_{p} on these crystals, a peculiar heat anomaly was observed at T_{INC} recently [10, 12], but no anomaly was observed near T_{LOW} [10]. Furthermore, there is no useful information about C_{p} on ST,

as long as we know. In this paper, we investigate in detail the specific heat on the single crystals of $\text{Sr}_2\text{Nb}_2\text{O}_7$, $\text{Sr}_2\text{Ta}_2\text{O}_7$ and $(\text{Sr}_{1-x}\text{Ba}_x)_2\text{Nb}_2\text{O}_7$ with $x < 2\%$, in a wide temperature range of 2–600 K.

Experimental

The single crystals were grown in an O_2 flow by a floating zone method using a FZ furnace (Crystal systems Inc). The starting materials were SrCO_3 (99.9%), BaCO_3 (99.9%), Nb_2O_5 (99.98%) and Ta_2O_5 (99.98%). Heat capacity was measured using two types of equipment: a fully automated measurement system of relaxation heat capacity (Quantum Design, a heat capacity module of PPMS) and an AC calorimeter (ULVAC, ACC1-M/L). They were used in a temperature range of 2–250 and 200–600 K, respectively. For the heat capacity measurement using PPMS, a single crystal with weight of about 20 mg was put with apiezon L grease on the sample stage. For the AC calorimeter, a thin plate-like crystal prepared by cleavage was attached to an E type thermocouple with a diameter of 20 μm using a silver paste. A heat capacity anomaly by the E type thermocouple at 410 K was removed numerically after the measurement.

Results and discussion

Specific heat C_{p} vs. T curves, measured on the single crystals of SN and ST, are shown in Figs 1 and 2, respectively. The C_{p} is composed of two kinds of data obtained by PPMS below 250 K and by an AC calo-

* Author for correspondence: akishige@edu.shimane-u.ac.jp

rimeter above 230 K. Because the AC calorimeter gives only relative values of C_p , the absolute values were determined as the data of the AC calorimeter coincide with those of PPMS in a temperature range of 230–250 K. A broad anomaly of the specific heat is seen around T_{INC} on SN (the inset of Fig. 1); similarly, a typical λ -type anomaly is seen around T_{SL} on ST (the inset of Fig. 2). However, at the temperatures below 300 K, we cannot see any heat anomalies on the both crystals of SN and ST (Figs 1 and 2, respectively).

For estimating excess specific heat ΔC_p caused by the phase transition, we must draw a baseline that is the normal portion of the specific heat. The solid lines in Figs 1 and 2 were obtained on an assumption that a polynomial function holds for $C_p(\text{base})$ in a limited temperature range of 260–590 K for SN, and of 300–465 K for ST: $C_p(\text{base})=a+bT+cT^2+dT^3+eT^4$, where a , b , c , d and e are constants. These constants were calculated by the method of least squares fitting to the data in the ranges of 260–360 and 530–590 K for SN, and in the ranges of 260–350 and 455–465 K for ST.

The obtained excess specific heats, $\Delta C_p=C_p-C_p(\text{base})$, for the two phase transitions at T_{INC} and T_{SL} are shown together in Fig. 3 for comparison. As seen in the figure, the incommensurate phase transition shows broad change over a wide temperature region of 350–520 K. By contrast, the super-lattice transition shows a relatively sharp change in comparison with that of T_{INC} ; the maximum value of ΔC_p reaches about $11 \text{ J mol}^{-1} \text{ K}^{-1}$ and the phase transition occurs in a rather narrow temperature region of 350–460 K. These relatively broad and continuous behaviors near the transition temperatures indicate

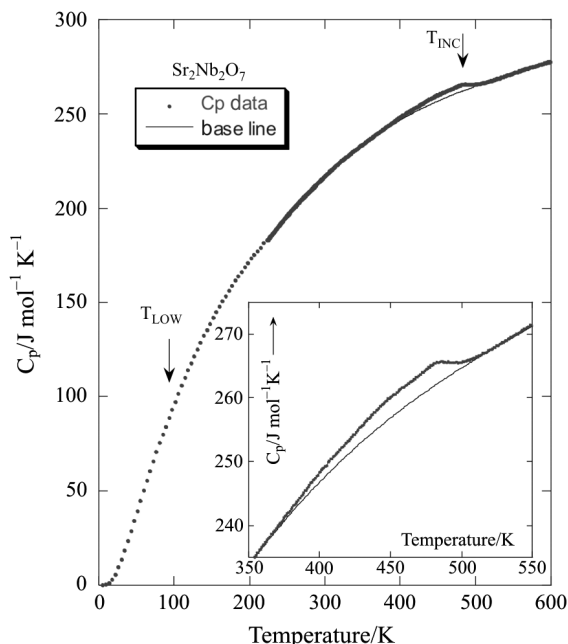


Fig. 1 Specific heat C_p on the $\text{Sr}_2\text{Nb}_2\text{O}_7$ single crystal

that the both transitions at T_{INC} and T_{SL} are of the second order.

The ΔC_p vs. T curves have small bumps near 410 K (Fig. 3). They are probably due to a heat anomaly of the E-type thermocouple used in this experiment. Most of the thermocouple's anomaly was removed numerically from the raw data after the experiment, but a small anomaly would be able to remain if there were another heat anomaly near 410 K.

The transition enthalpy ΔH was calculated from the excess specific heat ΔC_p , as shown in Fig. 4. The transition temperature can be determined as an inter-

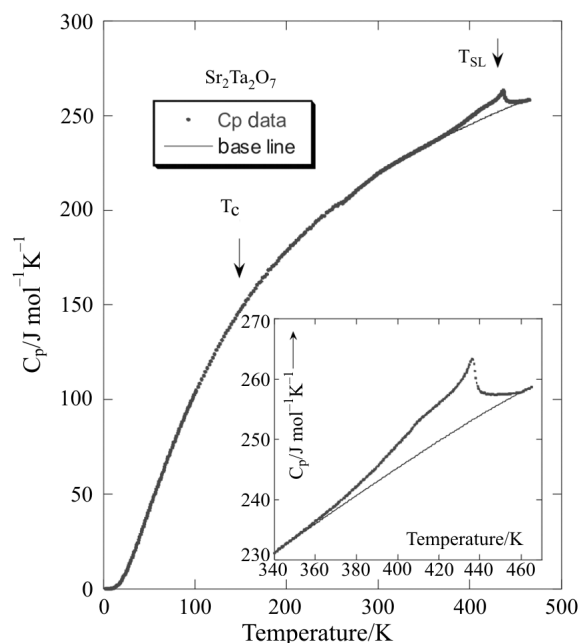


Fig. 2 Specific heat C_p on the $\text{Sr}_2\text{Ta}_2\text{O}_7$ single crystal

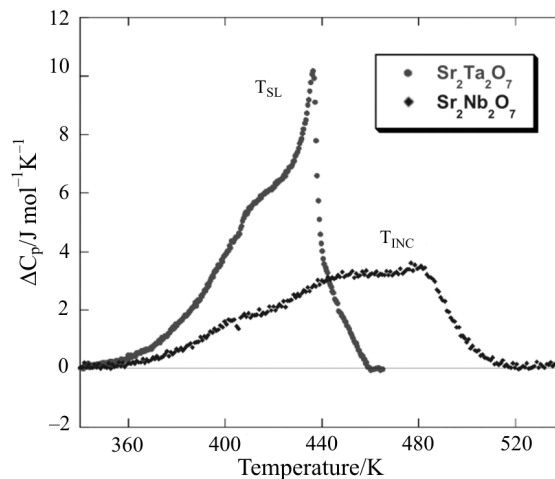


Fig. 3 Excess specific heat ΔC_p associated with the incommensurate phase transition at T_{INC} on SN and the super-lattice phase transition at T_{SL} on ST

section of the extrapolated lines of ΔH from the straight portions above and below the transition point: that is, T_{INC} and T_{SL} become 495 and 443 K, respectively. These values of the transition temperatures agree well with results of the dielectric constant [2, 8], the Raman scattering [13, 14], and the electron microscope [3]. The transition enthalpy ΔH and transition entropy ΔS are respectively estimated as $2.91 \cdot 10^2 \text{ J mol}^{-1}$ and $5.87 \cdot 10^{-1} \text{ J mol}^{-1} \text{ K}^{-1}$ for T_{INC} , and as $3.56 \cdot 10^2 \text{ J mol}^{-1}$ and $8.04 \cdot 10^{-1} \text{ J mol}^{-1} \text{ K}^{-1}$ for T_{SL} . These small values of the transition entropy may be attributed to that the phase transitions are a displacive type, as confirmed by existence of soft modes near T_{INC} and T_{SL} [13, 14].

Previously, Shabbir and Kojima reported the ΔC_p of SN [12], where they measured the heat capacity of SN using DSC. Curiously, their absolute values of C_p around T_{INC} are half of our results. Moreover, the data showed a sharp peak around 487 K, like as the ΔC_p of ST in Fig. 2. They estimated the transition entropy ΔS at T_{INC} as $0.71 \text{ J mol}^{-1} \text{ K}^{-1}$, which is a little larger than the present value of $\Delta S = 5.87 \cdot 10^{-1} \text{ J mol}^{-1} \text{ K}^{-1}$. Since the temperature resolution of AC calorimetry is higher than that of DSC in general, we must mention why the ΔC_p on SN in Fig. 1 does not show a sharp peak. In order to check this point, we measured C_p using several samples of SN, but all of our samples showed a broad anomaly at T_{INC} like Fig. 1. In our AC calorimetry, a thin crystal sample is attached to a thermocouple by a silver paste of small amounts, so that it may be possible that a kind of elastic strain induced by the contact gives unfavourable influence on the phase transition.

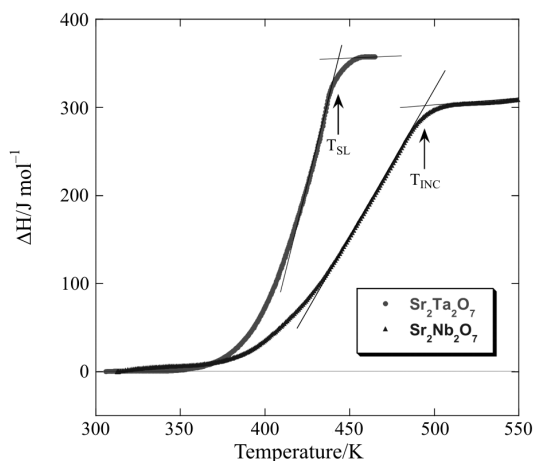


Fig. 4 Transition enthalpy ΔH associated with the incommensurate phase transition at T_{INC} on SN and with the super-lattice phase transition at T_{SL} on ST

	T/K	$\Delta H/\text{J mol}^{-1}$	$\Delta S/\text{J mol}^{-1} \text{ K}^{-1}$
T_{SL}	443	356	0.804
T_{INC}	495	291	0.587

In order to reveal the specific heat anomaly around T_{LOW} , we reinvestigated C_p on SN in detail. The C_p/T values on SN and ST are shown in Fig. 5 as a function of temperature. The specific heat of ST changes smoothly over the whole temperature range. Comparing the C_p vs. T curves between ST and SN, we can notice that C_p of ST is larger than that of SN at temperatures between 50 and 200 K and C_p of ST coincides with those of SN at temperatures below 30 and above 200 K. These differences of C_p between SN and ST at temperatures of 50–200 K are probably due to a broad and dispersive nature of the ferroelectric phase transition at $T_C = 166 \text{ K}$ on ST, as it is known that the dielectric constant of ST behaves like relaxor near T_C [8]. Another peculiar behavior is that SN shows a small jump of $\Delta C_p/C_p = 0.58\%$ at 95 K, as clearly shown in the inset of Fig. 5.

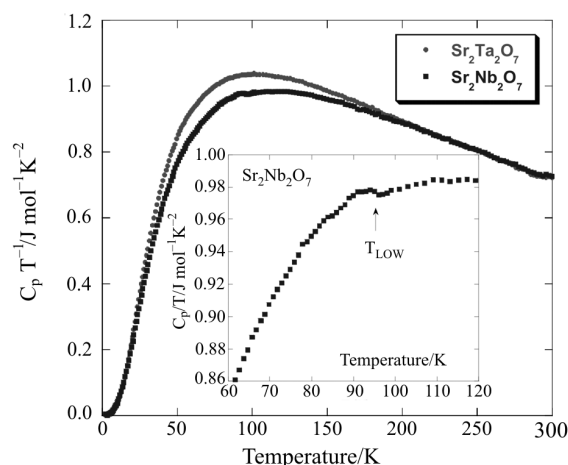


Fig. 5 C_p/T vs. T relations on $\text{Sr}_2\text{Nb}_2\text{O}_7$ and $\text{Sr}_2\text{Ta}_2\text{O}_7$ single crystals

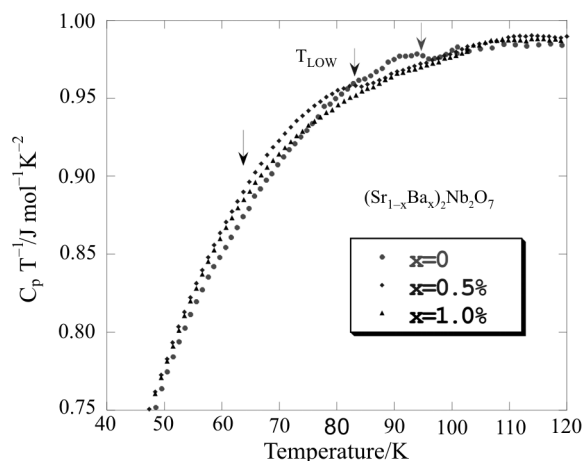


Fig. 6 C_p/T vs. T relations on $(\text{Sr}_{1-x}\text{Ba}_x)_2\text{Nb}_2\text{O}_7$ single crystals

Figure 6 shows the C_p/T behavior in the low temperature region for the Ba doped crystals,

($\text{Sr}_{1-x}\text{Ba}_x$) $_2\text{Nb}_2\text{O}_7$. As seen in the figure, the small jump at 95 K for $x=0\%$ decreases its temperature as the Ba content increases: the jump occurs at 83 K for $x=0.5\%$ and at 63 K for $x=1.0\%$. Above about $x=2\%$, we could not observe these small changes in C_p . These results agree well with our primitive results of the dielectric constant ϵ_b along the b -axis. The ϵ_b shows a peak around $T_{\text{LOW}} \approx 100$ K for $x=0$ crystals. The T_{LOW} decreases with increasing Ba content and disappears for $x=2\text{--}4\%$ crystals. Thus the small heat anomaly in Fig. 6 is certainly due to the phase transition at T_{LOW} .

Conclusions

Specific heats on the single crystals of $\text{Sr}_2\text{Nb}_2\text{O}_7$, $\text{Sr}_2\text{Ta}_2\text{O}_7$ and ($\text{Sr}_{1-x}\text{Ba}_x$) $_2\text{Nb}_2\text{O}_7$ were measured in a wide temperature range of 2–600 K. Specific heat anomalies were observed at the incommensurate phase transition of T_{INC} (=495 K) on $\text{Sr}_2\text{Nb}_2\text{O}_7$ and at the super-lattice phase transition of T_{SL} (=443 K) on $\text{Sr}_2\text{Ta}_2\text{O}_7$. The transition enthalpy ΔH and transition entropy ΔS were respectively estimated as $2.91 \cdot 10^2$ J mol $^{-1}$ and $5.87 \cdot 10^{-1}$ J mol $^{-1}$ K $^{-1}$ for T_{INC} , and as $3.56 \cdot 10^2$ J mol $^{-1}$ and $8.04 \cdot 10^{-1}$ J mol $^{-1}$ K $^{-1}$ for T_{SL} . A small heat anomaly was observed at the low temperature ferroelectric phase transition of T_{LOW} (=95 K) on $\text{Sr}_2\text{Nb}_2\text{O}_7$. The transition temperature T_{LOW} decreases with increasing Ba content x and vanishes around $x=2\%$.

Acknowledgements

This work was partly supported by the collaborative research project of Material and Structures Laboratory, Tokyo Institute

of Technology, and by a Grant-in-Aid for Scientific Research (No. 14340094) from the Japan Society for the Promotion of Science.

References

- 1 S. Nanamatsu, M. Kimura and T. Kawamura, *J. Phys. Soc. Jpn.*, 38 (1975) 817.
- 2 K. Ohi, M. Kimura, H. Ishida and H. Kakinuma, *J. Phys. Soc. Jpn.*, 46 (1979) 1387.
- 3 N. Yamamoto, K. Yagi, G. Honjo, M. Kimura and T. Kawamura, *J. Phys. Soc. Jpn.*, 48 (1980) 185.
- 4 N. Ishizawa, F. Marumo, T. Kawamura and M. Kimura, *Acta Crystallogr.*, B 31 (1975) 1912.
- 5 Y. Akishige, Y. Kobayashi, K. Ohi and E. Sawaguchi, *J. Phys. Soc. Jpn.*, 55 (1986) 2270.
- 6 V. Bobnar, P. Lunkenheimer, J. Hemberger, A. Loidl, F. Lichtenberg and J. Mannhart, *Phys. Rev.*, B 65 (2002) 155115.
- 7 Y. Fujimori, N. Izumi, T. Nakamura and A. Kamisawa, *Jpn. J. Appl. Phys.*, 37 (1998) 5207.
- 8 Y. Akishige and K. Ohi, *J. Phys. Soc. Jpn.*, 61 (1992) 1351.
- 9 N. Yamamoto, M. Nakamura, K. Yagi and K. Ohi, *J. Phys. Soc. Jpn.*, 49 Suppl. B (1980) 95.
- 10 Y. Akishige, M. Kamata and K. Fukano, *J. Korean Phys. Soc.*, 42 (2003) S1187.
- 11 A. Hushur, Y. Akishige and S. Kojima, *Ceramics International*, 30 (2004) 2023.
- 12 S. Shabbir and S. Kojima, *J. Phys. D: Appl. Phys.*, 36 (2003) 1036.
- 13 S. Kojima, M. Takashige, T. Nakamura, K. Ohi and H. Kakinuma, *Solid State Commun.*, 31 (1979) 755.
- 14 S. Kojima, K. Ohi and T. Nakamura, *Solid State Commun.*, 35 (1980) 79.

DOI: 10.1007/s10973-005-7076-y